nature medicine

MicroRNA-21 targets the vitamin D–dependent antimicrobial pathway in leprosy

Philip T Liu[1,2], Matthew Wheelwright[2], Rosane Teles[2], Evangelia Komisopoulou[3,4], Kristina Edfeldt[2], Benjamin Ferguson[2], Manali D Mehta[5], Aria Vazirnia[5], Thomas H Rea[6], Euzenir N Sarno[7], Thomas G Graeber[3,4,8–10] & Robert L Modlin[2,5]

Leprosy provides a model to investigate mechanisms of immune regulation in humans, given that the disease forms a spectrum of clinical presentations that correlate with host immune responses. Here we identified 13 miRNAs that were differentially expressed in the lesions of subjects with progressive lepromatous (L-lep) versus the self-limited tuberculoid (T-lep) disease. Bioinformatic analysis revealed a significant enrichment of L-lep–specific miRNAs that preferentially target key immune genes downregulated in L-lep versus T-lep lesions. The most differentially expressed miRNA in L-lep lesions, hsa-mir-21, was upregulated in *Mycobacterium leprae*–infected monocytes. By directly downregulating Toll-like receptor 2/1 heterodimer (TLR2/1)-induced *CYP27B1* and *IL1B* expression as well as indirectly upregulating interleukin-10 (IL-10), hsa-mir-21 inhibited expression of the genes encoding two vitamin D–dependent antimicrobial peptides, *CAMP* and *DEFB4A*. Conversely, knockdown of hsa-mir-21 in *M. leprae*–infected monocytes enhanced expression of *CAMP* and *DEFB4A* and restored TLR2/1-mediated antimicrobial activity against *M. leprae*. Therefore, the ability of *M. leprae* to upregulate hsa-mir-21 targets multiple genes associated with the immunologically localized disease form, providing an effective mechanism to escape from the vitamin D–dependent antimicrobial pathway.

© 2012 Nature America, Inc. All rights reserved.

npg

Interactions between the host immune response and the invading pathogen at the site of disease are crucial to the outcome of the infection. Leprosy, caused by the intracellular bacterium *M. leprae*, provides an extraordinary model for studying host-pathogen interactions in humans because the disease presents as a spectrum in which the clinical manifestations correlate with the level of immune response to the pathogen[1]. This allows for the investigation of the factors that contribute to the balance between host defense, persistence and pathogenesis at the site of disease in humans. At one end of the spectrum, in T-lep, the infection is self-limited, and skin lesions are typified by an adaptive immune response characterized by T helper type 1 (T_H1) cytokines[2,3] and an innate immune response characterized by macrophages programmed to express the vitamin D–mediated antimicrobial pathway[4]. At the other end of the spectrum, in L-lep, the infection is disseminated with lesions typified by an adaptive immune response characterized by T_H2 cytokines[2,3] and an innate immune response characterized by macrophages programmed to express a phagocytic activity[4]. To gain insight into the mechanisms that regulate host defense versus persistence in human infectious disease, we investigated miRNA expression in leprosy skin lesions.

RESULTS

Gene and miRNA profile in leprosy

The mRNA and miRNA expression profiles in skin lesions were determined in biopsy specimens from six individuals with T-lep and five individuals with L-lep collected at the time of diagnosis and classified according to the clinical and histopathological criteria of Ridley[1] (**Supplementary Fig. 1**). Unsupervised hierarchal clustering analysis of the mRNA profiles revealed two major groups in which the L-lep and T-lep samples were segregated (**Supplementary Fig. 2**). In contrast, hierarchal clustering analysis of the miRNA profiles performed on the same samples indicated two major miRNA patterns, with each group containing a mixture of both L-lep and T-lep samples (**Supplementary Fig. 2**). These results indicate that the principal component of the measured miRNA expression patterns in leprosy did not differentiate the lesion types.

To identify lesion-specific differences, we used a supervised approach. Differentially expressed miRNAs between the two clinical groups were identified by ranking miRNAs probes according to statistical significance (*t* test) and limited to sequences present in the miRBase database (version 14). There was a fivefold higher number

[1]Orthopaedic Hospital Research Center, University of California–Los Angeles, Los Angeles, California, USA. [2]Division of Dermatology, Department of Medicine, David Geffen School of Medicine, University of California–Los Angeles, Los Angeles, California, USA. [3]Crump Institute for Molecular Imaging, University of California–Los Angeles, Los Angeles, California, USA. [4]Department of Molecular and Medical Pharmacology, University of California–Los Angeles, Los Angeles, California, USA. [5]Department of Microbiology, Immunology and Molecular Genetics, University of California–Los Angeles, Los Angeles, California, USA. [6]Department of Dermatology, University of Southern California School of Medicine, Los Angeles, California, USA. [7]Leprosy Laboratory Institute Oswaldo Cruz, Rio de Janeiro, Brazil. [8]Institute for Molecular Medicine, University of California–Los Angeles, Los Angeles, California, USA. [9]Jonsson Comprehensive Cancer Center, University of California–Los Angeles, Los Angeles, California, USA. [10]California NanoSystems Institute, University of California–Los Angeles, Los Angeles, California, USA. Correspondence should be addressed to P.T.L. (ptliu@mednet.ucla.edu).

Received 29 December 2010; accepted 26 October 2011; published online 29 January 2012; doi:10.1038/nm.2584

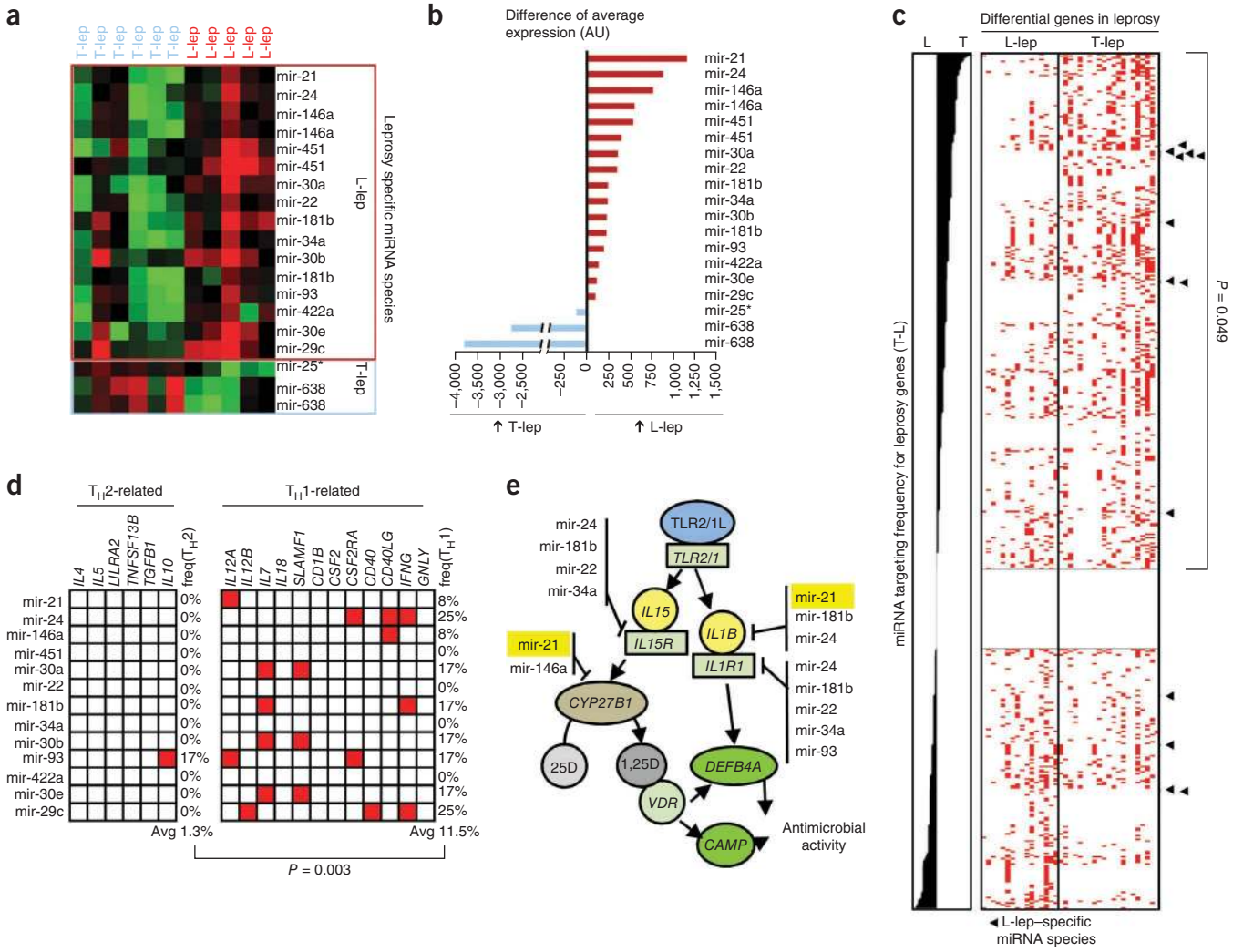

Figure 1 MiRNA expression and targeting profile in leprosy. (**a**,**b**) MiRNA probes that are differentially expressed between T-lep and L-lep lesions, depicted as normalized data (**a**) and raw expression values (**b**). AU, arbitrary units. (**c**) All miRNA species represented on the microarray platform ranged by targeting preference score. Arrowheads indicate L-lep–specific miRNA species. (**d**) Targeting preference of the L-lep– or T-lep–specific miRNA species for T_H2- or T_H1-related genes. Red boxes represent a predicted target site within the 3′ UTR of the indicated gene. (**e**) L-lep–specific miRNA species and predicted targeting of genes in the TLR2/1L-induced vitamin D–dependent antimicrobial pathway.

of differentially expressed miRNAs in the L-lep samples (16 probes representing 13 annotated miRNA species) versus the T-lep samples (three probes representing two unique miRNA species) (**Fig. 1a**). To compare the magnitude of differential expression between these miRNA species, we compared the un-normalized intensity values of the probes. The difference in intensity of the hsa-mir-21 probe was the greatest among the miRNA species differentially upregulated in L-lep versus T-lep lesions (**Fig. 1b**).

Targeting of immune genes by leprosy-specific miRNAs

Because the differentially expressed miRNA species were predominantly enriched in L-lep lesions, we hypothesized that regulation of miRNA expression at the site of the progressive disease inhibits expression of genes involved in host defense against the pathogen. We tested this hypothesis by integrating a prediction algorithm for miRNA binding sites in the 3′ untranslated regions (3′ UTRs) of mRNA species within curated sets of host immune response signature genes known to be differentially expressed in leprosy lesions, including T_H1- versus T_H2-related genes as well as the genes of the vitamin D pathway (**Supplementary Note**). All miRNA species represented on the microarray platform were ranked by their 'targeting preference score', calculated as the difference in frequency for targeting of the T-lep compared to L-lep signature genes (**Supplementary Fig. 3** and **Supplementary Note**). We next evaluated the enrichment of leprosy-disease-type–specific miRNA species by the Kolmogorov-Smirnov–based permutation test. On the basis of this analysis, we found the L-lep–specific miRNA species to be significantly associated with the miRNAs most strongly predicted to preferentially target T-lep signature genes ($P = 0.049$; **Fig. 1c**). Thus, L-lep–specific miRNAs may be a mechanism for the *M. leprae*–induced downregulation of T-lep host immune response signature genes in L-lep lesions.

In relation to the local immune response, the L-lep–specific set of miRNA species were predicted to have binding sites in the 3′ UTRs of T_H1-related signature genes, known to be differentially expressed in T-lep versus L-lep lesions, with an average targeting frequency of 11.5%. In contrast, the L-lep–specific set of miRNAs species showed a significantly ($P = 0.0003$) lower targeting frequency for T_H2-related genes, known to be differentially expressed in L-lep versus T-lep

© 2012 Nature America, Inc. All rights reserved.

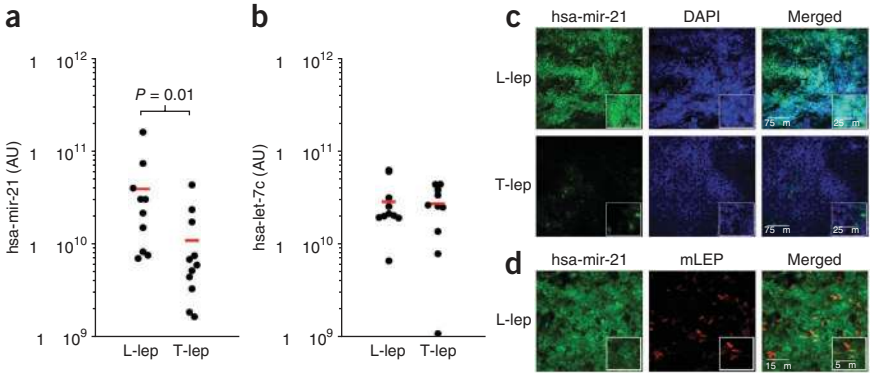

Figure 2 Expression of hsa-mir-21 in leprosy. (**a**,**b**) Expression levels of hsa-mir-21 (**a**) and hsa-let-7c (**b**) comparing L-lep versus T-lep lesions by qPCR. The levels of hsa-mir-21 and hsa-let-7c are normalized to 36B4 levels in the same tissue and depicted as values from individual lesions (filled circles) as well as the average (horizontal bars) of 10 L-lep lesions and 11 T-lep lesions. (**c**) Skin biopsy sections from subjects with L-lep or T-lep probed with a hsa-mir-21–specific oligomer using FISH. Cellular nuclei were visualized using DAPI. Data are representative experiment of four individual L-lep samples and three individual T-lep samples. (**d**) Skin biopsy section derived from subjects with L-lep and probed for hsa-mir-21 and *M. leprae* using FISH in conjunction with a monoclonal antibody specific for *M. leprae*, detected by confocal microscopy. The images are representative of three individual subjects.

lesions, with an average targeting frequency of 1.3% (**Fig. 1d**). Notably, multiple L-lep–specific miRNA species targeted two key genes in the vitamin D–dependent antimicrobial pathway, encoding cytochrome P450, family 27, subfamily B, polypeptide 1 (*CYP27B1*) and IL-1β (*IL1B*), but not the genes encoding the antimicrobial peptides induced by this pathway, cathelicidin (LL-37, encoded by *CAMP*) and defensin β4A (*DEFB4A*)[5,6] (**Fig. 1e**). Taken together, these results indicate that the L-lep–specific miRNAs target and potentially downregulate host defense genes in leprosy.

Regulation of hsa-mir-21 in leprosy

We verified the tissue expression of the most differentially expressed miRNA, hsa-mir-21, in L-lep lesions by real-time PCR (qPCR) and fluorescent *in situ* hybridization (FISH) in additional leprosy tissue sections. By qPCR, hsa-mir-21 levels were significantly higher (3.5-fold, $P = 0.01$) in 10 L-lep versus 11 T-lep lesions (**Fig. 2a**). An unrelated miRNA, hsa-let-7c, that was not differentially expressed in disease lesions by microarray analysis, was expressed at similar levels between the L-lep and T-lep lesions (**Fig. 2b**). Although the skin biopsies are composed predominately of granulomas in the dermis, we could not rule out that the differential expression of hsa-mir-21 came from nonimmune cells. Therefore, using FISH we determined that the frequency of hsa-mir-21–positive cells in the granulomatous regions was 25-fold higher in the L-lep lesions versus the T-lep lesions (98% versus 4% of nucleated cells, $P = 0.001$) (**Fig. 2c**). In the L-lep lesions, the hsa-mir-21–positive cells were located within the granulomas, in the same microanatomic locations as *M. leprae* (**Fig. 2d**). It was not possible to determine the frequency of cells expressing hsa-mir-21 and containing *M. leprae*, as these are found in distinct subcellular compartments: microRNAs are located in the cytoplasm and the pathogen resides within phagosomes. We used a scrambled probe as a negative control to demonstrate the absence of nonspecific binding in either lesion type (**Supplementary Fig. 4a**), and a positive control probe for the U6 noncoding small nuclear RNA showed equivalent RNA integrity (**Supplementary Fig. 4b**). Taken together, these three approaches, microarray, qPCR and FISH, provide evidence for the differential expression of hsa-mir-21 in L-lep versus T-lep lesions.

Given that we identified both *M. leprae* and hsa-mir-21 in the granulomas, we hypothesized that *M. leprae* induced hsa-mir-21 expression in monocytes and macrophages, the predominant cell type in a granuloma and the primary cell type infected by *M. leprae*. We infected human peripheral blood monocytes with live *M. leprae* at different multiplicities of infection (MOIs) for 18 and 40 h and measured hsa-mir-21 levels by qPCR. We efficiently infected monocytes with *M. leprae* (**Supplementary Fig. 5**), which triggered an upregulation of hsa-mir-21 in a dose-dependent and time-responsive manner, with a 4.1-fold change ($P = 0.005$) at 18 h and 7.6-fold change ($P = 0.00003$) at 40 h, both at an MOI of 10 (**Fig. 3a**). In contrast, *M. leprae* infection of monocytes did not result in detectable upregulation of hsa-let-7c (**Fig. 3b**).

To explore the mechanism by which *M. leprae* infection induces hsa-mir-21, we compared the ability of several key cell wall biomolecules to trigger hsa-mir-21 expression. Treatment of monocytes with phenolic glycolipid-I (PGL-I) induced a 2.9-fold increase in hsa-mir-21 expression, whereas the *M. leprae* lipoarabinomman (LAM) and lipomannan (LM), as well as a synthetic triacylated lipopeptide (a TLR2/1 ligand, TLR2/1L), did not significantly induce hsa-mir-21 (**Fig. 3c**). Together, these data indicate that hsa-mir-21 is present at the site of disease in leprosy, is associated with the progressive and disseminated form (L-lep) of the disease, is specifically induced in monocytes by *M. leprae* infection and is triggered by an *M. leprae*–specific glycolipid, PGL-I. It is therefore likely that *M. leprae* infection of macrophages induces the upregulation of hsa-mir-21 at the site of infection.

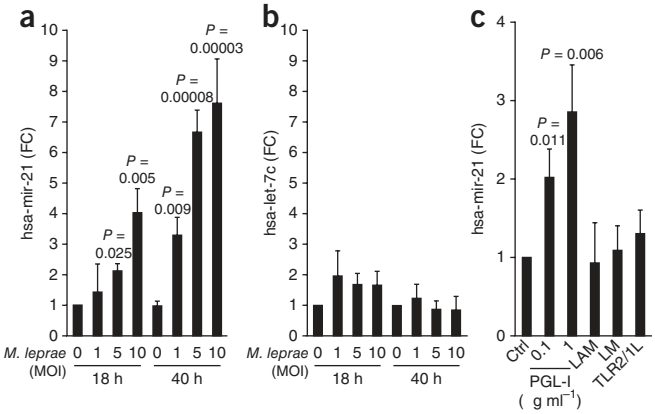

Figure 3 Regulation of hsa-mir-21 levels in primary human monocytes by *M. leprae*. (**a**,**b**) Levels of hsa-mir-21 (**a**) and hsa-let-7c (**b**) in primary human monocytes infected with *M. leprae* at an MOI of 0, 1, 5 or 10 for 18 h and 40 h. Data are mean fold change (FC) compared to no-infection control ± s.e.m., $n = 3$–5. (**c**) Levels of hsa-mir-21 in primary human monocytes after treatment with PGL-I, LAM (10 μg ml^{-1}), LM (10 μg ml^{-1}) or TLR2/1L for 18 h. Data are mean fold change compared to the vehicle control–treated cells ± s.e.m., $n = 3$–10.

© 2012 Nature America, Inc. All rights reserved.

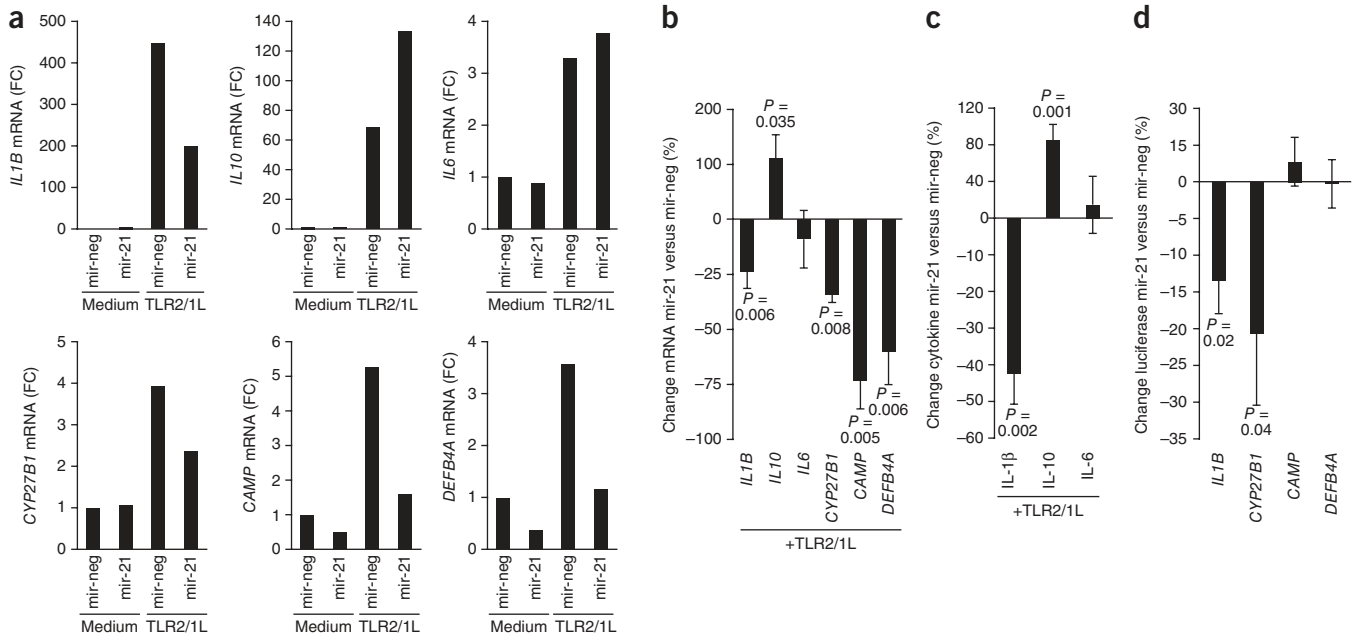

Figure 4 The ability of hsa-mir-21 to regulate the innate immune response in human monocytes. Primary human monocytes were transfected with the mature hsa-mir-21 (mir-21) oligomer or a nontargeting control (mir-neg) then treated with TLR2/1L for 18 h and 24 h. (**a**) Gene expression of *IL1B* at 18 h, *IL10* at 24 h, *IL6* at 16 h, *CYP27B1* at 16 h, *CAMP* at 24 h and *DEFB4A* at 24 h, as evaluated by qPCR. Data shown are representative experiments from more than five individual donors. (**b**) Change in gene expression comparing mir-21– to mir-neg–transfected cells after TLR2/1L simulation. Data are average percentage change mir-21 versus mir-neg ± s.e.m., $n = 3$–11. (**c**) Change in cytokine protein levels in culture supernatants comparing mir-21– to mir-neg–transfected cells after TLR2/1L stimulation. Data are average percentage change mir-21 versus mir-neg ± s.e.m., $n = 4$–6. Representative experiment is shown in **Supplementary Figure 6**. (**d**) Change in luciferase activity of cells co-transfected with a 3′ UTR luciferase reporter construct (*IL1B, CYP27B1, CAMP* or *DEFB4A*) and either mir-21 or mir-neg. Data are mean percentage change of each individual 3′ UTR construct comparing mir-21 versus mir-neg ± s.e.m., $n = 4$–6. Representative experiment is shown in **Supplementary Figure 8**.

© 2012 Nature America, Inc. All rights reserved.

Regulation of the vitamin D pathway by hsa-mir-21

It was noteworthy that of all the L-lep–specific miRNAs, only hsa-mir-21 had the potential to target both *IL1B* and *CYP27B1* (**Fig. 1e**), which are both required for TLR-induced, vitamin D–dependent expression of *CAMP* and *DEFB4A*[5,6]. We investigated the ability of hsa-mir-21 to regulate the expression of these antimicrobial genes by transfecting primary human monocytes with either the mature hsa-mir-21 oligomer or a nontargeting control oligomer, followed by activation with TLR2/1L. To determine the transfection efficiency of the miRNA oligomers into primary monocytes, we used a fluorescently tagged nontargeting control oligomer, which showed that 71% ($P = 0.002$) of the monocytes were miRNA positive (**Supplementary Fig. 6**). As a control for targeting specificity, we determined that overexpression of hsa-mir-21 downregulated interferon-γ–induced *IL12A* mRNA, a previously described direct target[7] (**Supplementary Fig. 7**). The presence of hsa-mir-21 during TLR2/1L activation of monocytes resulted in the downregulation of *IL1B* mRNA by 24% ($P = 0.006$, representative experiment in **Fig. 4a** and averaged in **Fig. 4b**). Despite the absence of predicted hsa-mir-21 target sites in the 3′ UTR of *IL10*, transfection of hsa-mir-21 enhanced TLR2/1-induced *IL10* mRNA levels by 110% ($P = 0.035$, **Fig. 4a**,**c**), consistent with studies in mouse cells[8]. In contrast, *IL6* mRNA, another cytokine without hsa-mir-21 target sequences, was not affected (**Fig. 4a**,**c**). TLR2/1-induced IL-1β secretion was reduced by 45% ($P = 0.003$), IL-10 release was enhanced by 85% ($P = 0.001$) and IL-6 levels did not change (representative experiment in **Supplementary Fig. 8** and averaged in **Fig. 4c**). Therefore, the effects of hsa-mir-21 on TLR2/1-induced cytokine mRNAs and secreted proteins were consistent.

Transfection of hsa-mir-21 also resulted in a 34% decrease in TLR-induced expression of CYP27B1 mRNA ($P = 0.008$, **Fig. 4a**,**b**). Given that hsa-mir-21 downregulated TLR2/1-induced IL-1β and CYP27B1 mRNA expression, we examined the effect of hsa-mir-21 on TLR2/1-induced antimicrobial peptide gene expression. Notably, TLR2/1 induction of *CAMP* and *DEFB4A* mRNAs was significantly inhibited by transfection of hsa-mir-21, by 73% ($P = 0.005$) and 60% ($P = 0.006$), respectively (**Fig. 4a**,**b**). Given that hsa-mir-21 upregulated IL-10, we investigated the effect of recombinant IL-10 on TLR2/1-induced gene expression. The addition of rIL-10 inhibited TLR2/1-induced mRNA expression of *CAMP* by 26% and *DEFB4A* by 35%, whereas the inhibition of *IL12B* was 76% (**Supplementary Fig. 9a**,**b**). Therefore, hsa-mir-21–mediated enhancement of IL-10 induction may partially contribute to the inhibition of antimicrobial gene expression.

We assessed whether hsa-mir-21 directly binds the TLR2/1-induced, vitamin D–dependent antimicrobial pathway genes with a 3′ UTR reporter assay. hsa-mir-21 directly bound the 3′ UTRs of both *CYP27B1* and *IL1B* but did not bind the 3′ UTRs of either *CAMP* or *DEFB4A* (**Fig. 4d**, **Supplementary Fig. 10** and **Supplementary Note**). These data indicate that hsa-mir-21 inhibits TLR2/1-mediated *CAMP* and *DEFB4A* expression directly by regulating key epigenetic targets including *CYP27B1* and *IL1B* and indirectly through induction of the immunomodulatory cytokine IL-10.

Role of hsa-mir-21 in the response to infection

Given the ability of hsa-mir-21 to downregulate key genes in the TLR2/1-induced antimicrobial pathway, and the observation that *M. leprae* induces hsa-mir-21 in monocytes, we investigated whether hsa-mir-21 contributes to inhibition of the innate immune response during *M. leprae* infection. We transfected monocytes with an hsa-mir-21–specific antisense oligomer (anti–mir-21), infected the transfected

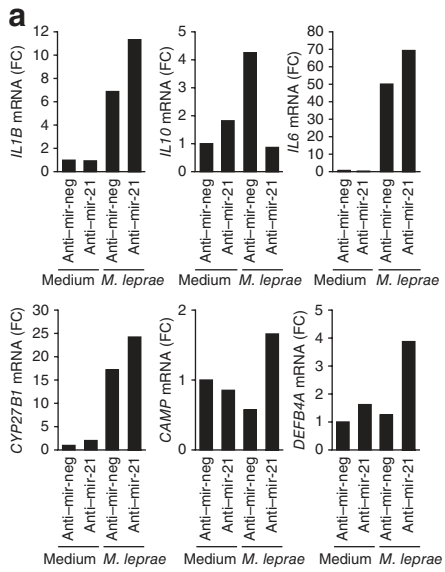

Figure 5 Role of hsa-mir-21 expression during *M. leprae* infection. Primary human monocytes were transfected with the antagomir against hsa-mir-21 (anti–mir-21) oligomer or a nonspecific control (anti–mir-neg) then infected with live *M. leprae* at an MOI of 10 for 18 h. Gene expression of *IL1B*, *IL10*, *IL6*, *CYP27B1*, *CAMP* and *DEFB4A* was evaluated by qPCR. (**a**) Representative experiments from more than four individual donors. (**b**) Change in gene expression comparing anti–mir-21– to anti–mir-neg–transfected cells following *M. leprae* infection for 18 h. Data are average percentage change anti–mir-21 versus anti–mir-neg ± s.e.m., $n = 4$–8.

monocytes with live *M. leprae*[9] for 18 h and then measured mRNA expression. The presence of anti–mir-21 (versus a control oligomer (anti–mir-neg), followed by *M. leprae* infection, resulted in a significant reduction of hsa-mir-21 levels by 70% ($P = 0.00002$, **Supplementary Fig. 11a**,**c**). Consistent with the hsa-mir-21 overexpression experiment, anti–mir-21 enhanced *IL12A* mRNA expression in the *M. leprae*–infected monocytes ($P = 0.006$, **Supplementary Fig. 11b**,**c**).

Relevant to the vitamin D–dependent innate immune pathway, anti–mir-21 increased *IL1B* mRNA expression in the *M. leprae*–infected monocytes by 118% ($P = 0.047$, **Fig. 5a**,**b**). In contrast, *IL10* mRNA was downregulated by 34% ($P = 0.045$), and there was no significant change in *IL6* mRNA levels (**Fig. 5a**,**b**). Notably, knockdown of hsa-mir-21 resulted in a significant increase in mRNA levels of *CYP27B1* (59%, $P = 0.014$), *CAMP* (100%, $P = 0.0006$) and *DEFB4A* (227%, $P = 0.014$) (**Fig. 5a**,**b**). These results provide evidence that monocytes and macrophages can detect *M. leprae* infection and trigger the vitamin D–dependent antimicrobial pathway; however, this response is inhibited by the pathogen's upregulation of hsa-mir-21.

Effects of hsa-mir-21 on innate antimicrobial activity

We investigated the role of hsa-mir-21 in regulating the TLR2/1-induced macrophage antimicrobial activity by overexpressing hsa-mir-21 during *Mycobacterium tuberculosis* infection. For these experiments, we used the avirulent *M. tuberculosis* H37Ra strain, as it does not contain a PGL-I homolog and failed to induce expression of hsa-mir-21 in monocytes upon infection (**Supplementary Fig. 12a**), despite induction of *IL6* mRNA in the same cells (**Supplementary Fig. 12b**). We transfected monocytes with hsa-mir-21 or a control oligomer, infected them with *M. tuberculosis* H37Ra overnight, subsequently treated them with TLR2/1L for 3 d and assessed bacterial viability by qPCR according to the ratio of 16S RNA to the IS6110 genomic repeat element DNA[10]. TLR2/1L induced an antimicrobial activity against *M. tuberculosis* in monocytes transfected with a control oligomer (**Fig. 6a**), at a level consistent with previous studies using the standard colony-forming unit assay (**Supplementary Note**)[6]. However, overexpression of hsa-mir-21 blocked the antimicrobial response and resulted in an increase in *M. tuberculosis* viability in TLR2/1L-activated cells (**Fig. 6a**). Also, in unstimulated cells, hsa-mir-21 increased bacterial viability. Overall, *M. tuberculosis* viability in TLR2/1L-treated as compared to control monocytes was significantly higher in the presence of hsa-mir-21 ($P = 0.01$, **Fig. 6b**).

To address the role of *M. leprae*–induced hsa-mir-21 in regulation of TLR2/1-induced antimicrobial activity, monocytes were transfected with anti–mir-21 or anti–mir-neg, then infected with live *M. leprae*. The transfected and infected cells were treated with the TLR2/1L for 3 d and antimicrobial activity assessed by qPCR by measuring the ratio of 16S RNA to RLEP DNA[10]. In anti–mir-neg transfected cells, TLR2/1-activation increased bacterial viability, consistent with previous findings indicating enhanced *M. tuberculosis* growth in TLR2/1-stimulated cells in the absence of *CAMP* and *DEFB4A*[6]. Strikingly, in anti–mir-21 transfected monocytes, TLR2/1-activation resulted in decreased bacterial viability (**Fig. 6c**). The anti–mir-21 oligomer had no effect on *M. leprae* viability in unstimulated monocytes (**Fig. 6c**).

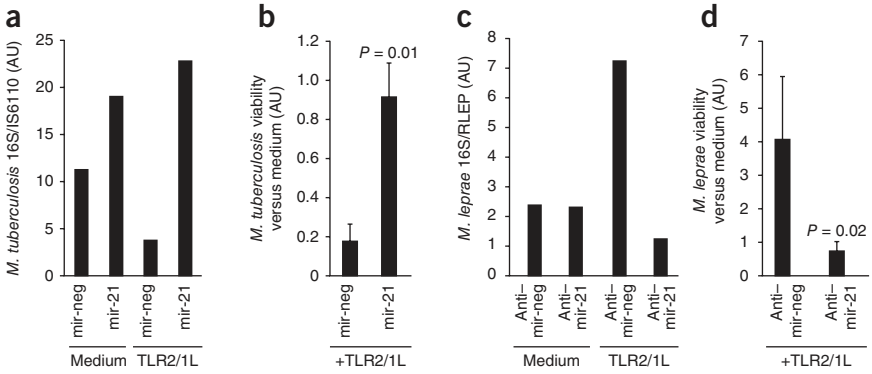

Figure 6 Role of hsa-mir-21 in TLR2/1-mediated antimicrobial activity. Primary human monocytes were transfected with the mature hsa-mir-21 (mir-21) oligomer or a nontargeting control (mir-neg) and then infected with live *M. tuberculosis* H37Ra at an MOI of 0.5 for 18 h. The monocytes were then treated with TLR2/1L (10 μg ml^{-1}) for 3 d. Levels of 16S rRNA and IS6110 DNA were assessed by qPCR. (**a**) The ratio of 16S rRNA to IS6110 DNA levels as a representative experiment from three donors. (**b**) Fold change in *M. tuberculosis* viability comparing TLR2/1L- versus medium-treated monocytes. Data are the mean fold change ± s.e.m., $n = 3$. Primary human monocytes were transfected with the antagomir against hsa-mir-21 (anti–mir-21) oligomer or a nonspecific control (anti–mir-neg) and then infected with live *M. leprae* at an MOI of 10 for 18 h. The monocytes were then treated with the TLR2/1L (10 μg ml^{-1}) for 3 d. Levels of 16S rRNA and RLEP DNA were assessed by qPCR. (**c**) Data are the ratio of 16S rRNA to RLEP DNA levels as a representative experiment from five donors. (**d**) Fold change in *M. leprae* viability comparing TLR2/1L– versus medium-treated monocytes. Data are the mean fold change ± s.e.m., $n = 5$.

© 2012 Nature America, Inc. All rights reserved.

In five donors tested, *M. leprae* viability in TLR2/1-stimulated cells was significantly lower in the presence of anti–mir-21 ($P = 0.02$, **Fig. 6d**). Together, the data from these infection experiments demonstrate the biologic relevance of hsa-mir-21 in innate host defense: the expression of hsa-mir-21 is sufficient to block TLR2/1-induced antimicrobial responses and the silencing of hsa-mir-21 induction restores TLR2/1-mediated antimicrobial activity.

DISCUSSION

Host-pathogen interactions determine the outcome of the immune response to microbial infection. Our data provide evidence that the human pathogen *M. leprae* regulates the miRNA profile at the site of infection in humans with leprosy and interferes with the host antimicrobial response. We used a unique bioinformatic strategy, combining an enrichment analysis of leprosy-disease-type–specific miRNA species ranked by 3′ UTR mRNA targeting preference and evaluated by the Kolmogorov-Smirnov-based permutation test. Together, these analyses led to the identification of hsa-mir-21 as differentially expressed in the progressive L-lep form of leprosy, with the potential to target genes in the vitamin D antimicrobial pathway. Infection of human monocytes with live *M. leprae,* or treatment with the mycobacterial virulence factor PGL-I, induced expression of hsa-mir-21. Next, we showed that hsa-mir-21 functionally downregulates the TLR2/1-induced vitamin D antimicrobial pathway by directly targeting *CYP27B1* and *IL1B* and indirectly inducing IL-10, all leading to the inhibition of the antimicrobial peptides *CAMP* and *DEFB4A*. Silencing of hsa-mir-21 during *M. leprae* infection led to the enhanced expression of vitamin D pathway genes. Finally, introduction of hsa-mir-21 into monocytes was sufficient to block TLR2/1-induced antimicrobial activity against *M. tuberculosis*, and the silencing of hsa-mir-21 induction restored TLR2/1-mediated antimicrobial activity against *M. leprae.* Therefore, these data identify an evasion strategy in which a microbial pathogen regulates the host miRNA profile at the site of infection to inhibit the antimicrobial response.

Although *M. leprae* was the first human pathogen discovered[11], it still cannot be grown in the laboratory, providing a major obstacle to investigation of the immunology of leprosy. To our knowledge, it has not been possible to demonstrate immune-mediated antimicrobial activity against *M. leprae* in primary human cells[12]. A previous comparison of antimicrobial responses in mouse and human macrophages demonstrated that the combination of lipopolysaccharide and interferon-γ reduced the viability of intracellular *M. leprae* in mouse but not human macrophages[12]. Here we successfully demonstrate that immune activation of *M. leprae*–infected human monocytes decreases bacterial viability, finding that TLR2/1 activation induced a fourfold reduction in *M. leprae* viability only when hsa-mir-21 was silenced. In addition, overexpression of hsa-mir-21 blocked the TLR2/1-induced antimicrobial activity against *M. tuberculosis*, resulting in a fivefold increase in bacterial viability. Taken together, these data indicate the biological relevance of hsa-mir-21 in the host antimicrobial response.

We gained insight into the mechanism by which *M. leprae* induces a specific miRNA immune regulatory profile at the site of infection by finding that hsa-mir-21 was induced in monocytes after *M. leprae* infection or by treatment with *M. leprae*–derived PGL-I. Previously, PGL-I has been shown to inhibit monocyte responses[13,14], as well as associate with mycobacterial virulence[15]. Further studies are needed to elucidate the mechanism of induction and functional role of those miRNAs differentially expressed in L-lep lesions. Given that the degree of genetic diversity in *M. leprae* clinical isolates is not as broad as compared with other human pathogens[16], it is not likely that species subtypes differentially induce single miRNAs, as has been shown for *Francisella tularensis*[17]. To complement the study of miRNA profiles in disease lesions as shown here, additional insight can be obtained by profiling the miRNAs induced by a pathogen in an isolated cell type[18]. It should be possible to learn whether the ability of a pathogen to induce a single miRNA or set of miRNA species that targets and inhibits host immune responses provides a potential virulence mechanism that contributes to the pathogenesis of infectious disease[19].

Our data demonstrate that a single miRNA species, by both directly and indirectly regulating immune modulatory genes, can affect the downstream effectors of an innate immune–triggered antimicrobial pathway. Specifically, hsa-mir-21 inhibited TLR2/1-induced *CYP27B1* and *IL1B* gene expression and enhanced IL-10 expression, thereby preventing upregulation of the *CAMP* and *DEFB4* mRNAs, which encode antimicrobial peptides. These factors are all key to the outcome of the vitamin D antimicrobial pathway: (i) CYP27b1 converts vitamin D from an inactive to active state, leading to antimicrobial activity, (ii) IL-1β is required for DEFB4 induction and (iii) IL-10 is known to inhibit TLR-induced responses[20]. Consequently, hsa-mir-21 inhibits the innate immune response by its distinct gene regulatory activities: the indirect upregulation of an immunosuppressive cytokine and direct targeting of epigenetic components required for the TLR-induced, vitamin D–dependent antimicrobial pathway[5,6]. Consistent with this model, the genes directly targeted by hsa-mir-21, *CYP27B1* and *IL1B*, are downregulated in L-lep versus T-lep lesions[2,4]. Although the relationship between expression of miRNAs and gene targets in disease lesions is correlative, the demonstration that hsa-mir-21 is induced in human primary monocytes 18 h after *M. leprae* infection and its effect on the TLR-induced antimicrobial response suggest a role in disease pathogenesis. Our investigation of the effect of a single miRNA in leprosy provides a framework for analyzing the set of miRNAs that are differentially expressed at the site of disease to determine their cumulative role in regulating the host immune response, including autophagy and antimicrobial pathways.

The ability of anti–mir-21 to enhance the vitamin D–dependent antimicrobial pathway provides a potential therapeutic strategy to intervene in human infectious disease. In leprosy, the vitamin D antimicrobial pathway may contribute to disease outcome, on the basis of the preferential expression of antimicrobial pathway genes in the T-lep versus L-lep form[4], the correlation of the vitamin D receptor single-nucleotide polymorphism in humans with L-lep[21] and the reported successful use of vitamin D as a therapeutic adjuvant in the treatment of leprosy[22]. Potentially, the combination of vitamin D supplementation with targeted miRNA therapy could provide an optimal treatment approach to leprosy and other chronic infectious diseases in which the cellular immune response is dysregulated. This type of approach may be particularly worth exploring in the clinical setting of drug-resistant pathogens, including multi-drug-resistant, extremely drug-resistant and totally drug-resistant tuberculosis, in which antimicrobial therapy is losing its effectiveness. Finally, our findings may be relevant to other diseases, including infectious[23,24], autoimmune[25] and neoplastic[26,27] diseases in which vitamin D sufficiency has been shown to be required for optimal host immunity.

METHODS

Methods and any associated references are available in the online version of the paper at http://www.nature.com/naturemedicine/.

© 2012 Nature America, Inc. All rights reserved.

Accession codes. Accession numbers for genes, miRNAs, mRNA arrays and miRNA arrays are provided in **Supplementary Table 1**.

Note: Supplementary information is available on the Nature Medicine website.

ACKNOWLEDGMENTS

We would like to thank G. Cheng, R. O'Connell, J. Krahenbuhl, R. Lahiri and B. Bloom for their helpful discussions. The live *M. leprae* was provided by the US National Hansen's Disease Programs through the generous support of the American Leprosy Missions and Society of St. Lazarus of Jerusalem. This work was supported by US National Institutes of Health grants AI 022553, AI 047868, AR 040312 and AI 073539. P.T.L. is supported by US National Institutes of Health K22 Career Development Award AI 85025. K.E. is supported by a postdoctoral grant from the Wenner-Gren Foundations (Sweden). We would like to thank M. Schibler and the University of California–Los Angeles, California NanoSystems Institute, Advanced Light Microscopy Core Facility for their assistance with the confocal studies.

AUTHOR CONTRIBUTIONS

P.T.L. performed the experiments, supervised the project, analyzed the data and wrote the manuscript. M.W. performed the *in situ* hybridization experiments and a portion of the *M. leprae* infection, antimicrobial and monocyte transfection experiments. R.T. performed the microarray experiments. E.K. performed the bioinformatics analysis of the microarray data. K.E. performed the IL-10–related experiments. B.F. performed a portion of the *M. leprae* infection, antimicrobial and monocyte transfection experiments. M.D.M. performed a portion of the *M. leprae* infection and ligands experiments. A.V. performed a portion of the monocyte transfection experiments. T.H.R. and E.N.S. diagnosed patients with leprosy collected skin biopsy specimens. T.G.G. designed, supervised and performed bioinformatics analysis. R.L.M. supervised the project and wrote the manuscript.

COMPETING FINANCIAL INTERESTS

The authors declare no competing financial interests.

Published online at http://www.nature.com/naturemedicine/.
Reprints and permissions information is available online at http://www.nature.com/reprints/index.html.

1. Ridley, D.S. & Jopling, W.H. Classification of leprosy according to immunity. A five-group system. *Int. J. Lepr. Other Mycobact. Dis.* **34**, 255–273 (1966).
2. Yamamura, M. *et al.* Defining protective responses to pathogens: cytokine profiles in leprosy lesions. *Science* **254**, 277–279 (1991).
3. Salgame, P. *et al.* Differing lymphokine profiles of functional subsets of human CD4 and CD8 T cell clones. *Science* **254**, 279–282 (1991).
4. Montoya, D. *et al.* Divergence of macrophage phagocytic and antimicrobial programs in leprosy. *Cell Host Microbe* **6**, 343–353 (2009).
5. Liu, P.T. *et al.* Toll-like receptor triggering of a vitamin D–mediated human antimicrobial response. *Science* **311**, 1770–1773 (2006).
6. Liu, P.T. *et al.* Convergence of IL-1β and VDR activation pathways in human TLR2/1-induced antimicrobial responses. *PLoS ONE* **4**, e5810 (2009).
7. Lu, T.X., Munitz, A. & Rothenberg, M.E. MicroRNA-21 is up-regulated in allergic airway inflammation and regulates IL-12p35 expression. *J. Immunol.* **182**, 4994–5002 (2009).
8. Sheedy, F.J. *et al.* Negative regulation of TLR4 via targeting of the proinflammatory tumor suppressor PDCD4 by the microRNA miR-21. *Nat. Immunol.* **11**, 141–147 (2010).
9. Adams, L.B. *et al.* The study of *Mycobacterium leprae* infection in interferon-γ gene–disrupted mice as a model to explore the immunopathologic spectrum of leprosy. *J. Infect. Dis.* **185** (suppl. 1), S1–S8 (2002).
10. Martinez, A.N. *et al.* Molecular determination of *Mycobacterium leprae* viability by use of real-time PCR. *J. Clin. Microbiol.* **47**, 2124–2130 (2009).
11. Hansen, G.A. Undwersogelser angaende spedalskhedens arsager. *Norsk. Mag. Laegevid* **4**, 1–88 (1874).
12. Peña, M.T. *et al.* Expression and characterization of recombinant interferon γ (IFN-γ) from the nine-banded armadillo (*Dasypus novemcinctus*) and its effect on *Mycobacterium leprae*–infected macrophages. *Cytokine* **43**, 124–131 (2008).
13. Vachula, M., Holzer, T.J. & Andersen, B.R. Suppression of monocyte oxidative response by phenolic glycolipid I of *Mycobacterium leprae*. *J. Immunol.* **142**, 1696–1701 (1989).
14. Neill, M.A. & Klebanoff, S.J. The effect of phenolic glycolipid-1 from *Mycobacterium leprae* on the antimicrobial activity of human macrophages. *J. Exp. Med.* **167**, 30–42 (1988).
15. Tabouret, G. *et al. Mycobacterium leprae* phenolglycolipid-1 expressed by engineered *M. bovis* BCG modulates early interaction with human phagocytes. *PLoS Pathog.* **6**, e1001159 (2010).
16. Clark-Curtiss, J.E. & Walsh, G.P. Conservation of genomic sequences among isolates of *Mycobacterium leprae*. *J. Bacteriol.* **171**, 4844–4851 (1989).
17. Cremer, T.J. *et al.* MiR-155 induction by *F. novicida* but not the virulent *F. tularensis* results in SHIP down-regulation and enhanced pro-inflammatory cytokine response. *PLoS ONE* **4**, e8508 (2009).
18. Liu, Z. *et al.* Up-regulated microRNA-146a negatively modulate *Helicobacter pylori*–induced inflammatory response in human gastric epithelial cells. *Microbes Infect.* **12**, 854–863 (2010).
19. Sinsimer, D. *et al. Mycobacterium leprae* actively modulates the cytokine response in naive human monocytes. *Infect. Immun.* **78**, 293–300 (2010).
20. Krutzik, S.R. *et al.* Activation and regulation of Toll-like receptors 2 and 1 in human leprosy. *Nat. Med.* **9**, 525–532 (2003).
21. Roy, S. *et al.* Association of vitamin D receptor genotype with leprosy type. *J. Infect. Dis.* **179**, 187–191 (1999).
22. Herrera, G. Vitamin D in massive doses as an adjuvant to the sulfones in the treatment of tuberculoid leprosy. *Int. J. Lepr.* **17**, 35–42 (1949).
23. Rook, G.A.W. The role of vitamin D in tuberculosis. *Am. Rev. Respir. Dis.* **138**, 768–770 (1988).
24. Crowle, A.J., Ross, E.J. & May, M.H. Inhibition by 1,25(OH)2-vitamin D3 of the multiplication of virulent tubercle bacilli in cultured human macrophages. *Infect. Immun.* **55**, 2945–2950 (1987).
25. Munger, K.L., Levin, L.I., Hollis, B.W., Howard, N.S. & Ascherio, A. Serum 25-hydroxyvitamin D levels and risk of multiple sclerosis. *J. Am. Med. Assoc.* **296**, 2832–2838 (2006).
26. Lappe, J.M., Travers-Gustafson, D., Davies, K.M., Recker, R.R. & Heaney, R.P. Vitamin D and calcium supplementation reduces cancer risk: results of a randomized trial. *Am. J. Clin. Nutr.* **85**, 1586–1591 (2007).
27. Ahn, J. *et al.* Vitamin D–related genes, serum vitamin D concentrations and prostate cancer risk. *Carcinogenesis* **30**, 769–776 (2009).

© 2012 Nature America, Inc. All rights reserved.

ONLINE METHODS

Statistical analyses. Percentage change due to miRNA or antagomir was analyzed against no change with an unpaired Student's *t* test. Gene or miRNA induction studies were analyzed with an unpaired Student's *t* test against the medium control of each experiment. L-lep–specific miRNA targeting of T_H1- and T_H2- related genes was analyzed with an unpaired Student's *t* test. The miRNA targeting preference was determined with the Kolmogorov-Smirnov–based permutation analysis as noted in the **Supplementary Note**. Error bars represent the s.e.m. between individual donor values.

Leprosy biopsy specimens. The acquisition of all specimens was approved by the Medical Investigational Review Board 1 (MIRB1) of the University of California–Los Angeles; more details can be found in the **Supplementary Methods**. Scalpel or punch skin biopsy specimens were obtained after informed consent from individuals with tuberculoid leprosy and individuals with lepromatous leprosy at the time of diagnosis; therefore, all samples are representative of untreated disease.

Microarray analysis. For gene and miRNA expression profiling, the RNA from skin biopsy specimens was processed and analyzed by the University of California–Los Angeles Clinical Microarray Core Facility using the Affymetrix U133 Genechip and Asuragen using the Discovarray platform, respectively. Additional details pertaining hierarchical clustering, cluster dendrograms and heat maps are included in the **Supplementary Methods**.

***In situ* hybridization.** Leprosy skin biopsy specimens were snap frozen and sectioned to a thickness of 10 µm and then mounted onto a glass slide. The protocol has been previously described[28] and adapted for current use. Briefly, biotinylated hsa-mir-21–specific, U6–specific and nonspecific control probes were purchased (Exiqon) and hybridized to the tissue at 0.1 pg μl^{-1} for 1–4 h, followed by incubation with Streptavidin–horseradish peroxidase. Then, the sections were incubated with the TSA Plus Fluorescein System (PerkinElmer) according to the manufacturer's instructions. A coverslip was sealed to the slides with ProLong Gold with DAPI (Invitrogen), left to dry at 4 °C in the dark overnight and imaged using a Leica FLIM confocal microscope (Leica).

Live *Mycobacterium leprae*. Live and viable *M. leprae* bacteria were generously donated by J.L. Krahenbuhl. Additional information is included in the **Supplementary Methods**.

Quantitative PCR. For miRNA analysis, qPCR was performed using the TaqMan MicroRNA Cells-to-CT kit in conjunction with the TaqMan MicroRNA Assay for hsa-mir-21 (Applied Biosystems) or the NCODE miRNA cDNA Synthesis and qPCR Kit (Invitrogen) according to the manufacturers' recommended conditions. For mRNA studies, total RNA was isolated from monocytes by TRIzol (Invitrogen), and cDNA libraries were made using the iScript cDNA synthesis kit (BioRAD). qPCR reactions were carried out using the iQ SYBR Green qPCR Master Mix (BioRAD) according to the manufacturer's recommended conditions. The primer sequences for *36B4*, *CAMP*, *DEFB4A* and *CYP27B1* were previously published[5,6]; other primer sequences and calculations are included in the **Supplementary Methods**.

Transfection of monocytes. Monocytes were enriched from peripheral blood mononuclear cells using a Percoll (GE Healthcare) gradient as previously described[6] and then transfected with either the mature miRNA or the antagomir oligomers using the Amaxa Nucleofector system with the Human Monocyte Nucleofector transfection kit (Lonza) according to the manufacturer's recommended protocol. Additional details are included in the **Supplementary Methods**.

miRNA direct targeting analysis. MiRNA-targeting plasmids were prepared with endotoxin-free conditions using the Qiagen Endofree Maxi Kit (Qiagen) according to the manufacturer's recommended protocols. The constructs were co-transfected into HEK293 cells (ATCC) with either hsa-mir-21 mature oligomer or a nontargeting control oligomer with the Amaxa Nucleofector Transfection Cell Line V kit (Lonza) according to the manufacturer's optimized protocol. After transfection, the cells were rested for 2 h and then washed to replace the medium. The transfected cells were then incubated 37 °C for 16 h, and luciferase activity was measured using the Dual Glo-Luciferase Assay System (Promega) according to the manufacturer's recommended protocols. The miRNA effect is calculated as a ratio of the firefly to *Renilla* luciferase activities.

Antimicrobial assays. To assess *M. leprae* and *M. tuberculosis* H37Ra viability from infected macrophages, we adapted the previously described real-time PCR–based method for the assessment of bacterial viability, which compares 16S RNA levels to levels of a genomic DNA as a predictor of bacterial viability (**Supplementary Note**)[10]. Experimental details are included in the **Supplementary Methods**. The 16S and bacterial DNA values were calculated using the $\Delta\Delta C_T$ analysis, with the bacterial DNA value serving as the housekeeping gene. The *M. leprae* 16S and *M. leprae* repetitive genomic element primers used were as previously described[10]; other primer sequences are included in the **Supplementary Methods**.

Additional methods. Detailed methodology is described in the **Supplementary Methods**.

28. Silahtaroglu, A.N. *et al.* Detection of microRNAs in frozen tissue sections by fluorescence *in situ* hybridization using locked nucleic acid probes and tyramide signal amplification. *Nat. Protoc.* **2**, 2520–2528 (2007).

© 2012 Nature America, Inc. All rights reserved.

doi:10.1038/nm.2584